MEASUREMENT OF SURFACE FLOW VELOCITY OF ACTIVE ROCK GLACIERS USING ORTHOPHOTOS OF VIRTUAL GLOBES

Viktor KAUFMANN[1]

ABSTRACT:
In this paper we demonstrate how multi-temporal high-resolution orthophotos taken from virtual globes, such as Google Maps and Microsoft Bing Maps, can be used not only for the detection of active rock glaciers but also for the precise measurement of flow/creep velocities. Our study area covers the central and western part of the Schober Mountains, which belongs to the Hohe Tauern range of the Austrian Alps. The present paper is focused on three active rock glaciers, i.e. Leibnitzkopf, Tschadinhorn, and Ganot, which were identified and examined for the first time based on the above mentioned freely available image data. Two-dimensional flow/creep vector fields were determined using a Matlab-based toolbox developed at our Institute. Methods of both photogrammetry and computer vision were implemented to co-register the multi-temporal orthophotos and to precisely measure motion parallaxes with sub-pixel accuracy. The results obtained were visualized through vector plots, isotachs and computer animations. The accuracy of the displacement vectors was thoroughly checked at stable non-moving regions in the surroundings of the rock glaciers. The paper concludes with a summary of the pros and cons of the workflow outlined.

Keywords: *Google Maps, Microsoft Virtual Earth, rock glacier, monitoring, flow/creep velocity, visualization, Hohe Tauern range, Austria.*

1. INTRODUCTION

Rock glaciers are creep phenomena of mountain permafrost and are composed of rocks and interstitial ice (*Barsch, 1996*). Active rock glaciers creep downslope by force of gravity due to plastic deformation of the ice and also sliding occasionally at certain shear horizons. Their appearance is reminiscent of lava flows. Surface flow/creep velocity of rock glaciers and also its temporal change is of high relevance to environmental research because local climate (mean annual air temperature) is supposed to (positively) influence the former. Fast creeping rock glaciers (> 1 m/year) present a natural hazard because prevailing high strain rates may cause surface ruptures and disintegration of the rock/ice mixture, potentially triggering landslides and rockfalls. The movement of a rock glacier can be quantified by various measurement techniques. Image-based methods are widely used in rock glacier monitoring. Particle tracking in multi-temporal orthophotos using automatic image matching techniques is capable to generate area-wide dense fields of displacement vectors (= flow/creep vectors).

[1] *Institute of Remote Sensing and Photogrammetry, Graz University of Technology, Austria, viktor.kaufmann@tugraz.at.*

2. IMAGE-BASED MEASUREMENT OF HORIZONTAL FLOW/CREEP VECTOR FIELDS

Different measurement methods of displacement vectors of the Earth's surface exist. Among them, remote sensing is a very powerful technique for retrieving metric information of surface change. An outline of the different methods applied to glaciers and permafrost creep is given, for example, in *Kääb (2005)*. Image-based measurement of horizontal (two-dimensional/2-D) displacement vectors using multi-temporal orthophotos/ortho-images is relatively easy because rectified image data – ortho-images are orthogonal projections of the Earth's surface texture into a horizontal reference plane – do not show any geometric distortions due to relief and imaging geometry as compared to the original image data acquired by the imaging sensor. This specific geometric property facilitates the automatic measurement (tracking) of distinct points by digital image matching techniques (cp. also *Baltsavias, 1994*).

The present study is based on area-based image matching using normalized cross correlation (NCC) as a similarity measure for finding conjugate positions. The method (for details see *Bischof and Leberl, 2004*) performs generally quite well if the photo/image patches (= template and search windows) to be compared with are geometrically similar, i.e., image rotation and scale difference are reasonably small. The computation of NCC coefficient compensates for differences in brightness and contrast of the template and the search window, which is particularly advantageous if images were taken at different dates and time.

A Matlab-based toolbox for automatic measurement of 2-D displacement vectors in digital photo/image pairs has been developed at the author's Institute. Candidate points in the reference image (of epoch T1) can be selected in threefold manner, i.e., manually, applying interest operators such as Förstner or Harris, or specifying points on a regular grid. The size of the template window can be set interactively according to the signal-to-noise ratio in the images. Computational speed does not only depend on the size of the template window but also on good estimates of the corresponding points in the second image (of epoch T2). The maximum of NCC coefficient is found by "non-maxima suppression" technique. Sub-pixel interpolation is done by curve (parabola) fitting. Quality control of image matching is carried out through thresholding NCC coefficients and back matching, the latter being very efficient in avoiding wrong registrations. Remaining gross errors (blunders) are detected visually based on certain criteria, such as smoothness of the vector field, known flow constraints, etc. In case that both the reference and the search image are not absolutely (geo-)referenced to a common co-ordinate system in terms of shift, co-ordinate offsets have to be determined at stable reference points. The accuracy of image matching (image registration) can be deduced directly from displacements measured at these stable points.

3. TEST SITES

3.1. Searching for active rock glaciers

Glacier and rock glacier studies have been carried out jointly by the Institute of Geography and Regional Science, University of Graz, and the Institute of Remote Sensing and Photogrammetry, Graz University of Technology, during almost three decades in the Schober group, Austria. The Schober group is located south of the main crest of the Hohe Tauern range and holds more than 30 peaks higher than 3000 m. Recent glaciation is sparse and limited to higher elevations. This mountain group is abundant in intact rock glaciers due its relief, geology, and regional climate. Until recently the main focus of the studies of the two Institutes was in the eastern part of the Schober group. Now the author has extended the interest also to the western part of the Schober group looking for very active rock glaciers. *Lieb (1986)* and *Buchenauer (1990)* can be recommended as a reference for permafrost related studies in the Schober group. Both authors have addressed the issue of rock glacier movement in their studies, however, metric quantification of the movement was not within the scope of their work.

By chance, the author noticed that both digital/virtual globes, i.e., Google Maps (*http://maps.google.at/*) and Microsoft Bing Maps (formerly Microsoft Virtual Earth, *http://www.bing.com/maps/*), which he was using for exploring this new region, used high-resolution aerial orthophotos of different acquisition dates as a backdrop for their digital maps. Because of the on-screen copyright display of the image data and the author's knowledge about available aerial photographs of this region, the original source of the image data and their acquisition dates could be revealed easily. The color photographs of Google Maps were taken on 18 September 2002 and those ones of Microsoft Bing Maps on 21 September 2006.

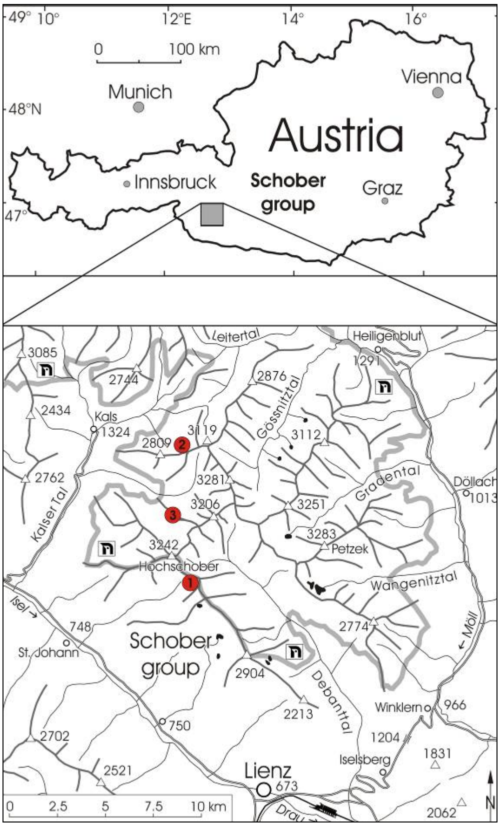

Fig. 1 Location map: ① Leibnitzkopf rock glacier, ② Tschadinhorn rock glacier, ③ Ganot rock glacier

The western part of the Schober group was screened for very active rock glaciers looking stereoscopically at potential sites as outlined in *Kaufmann (2009)*. The basic idea behind the procedure applied is that motion parallaxes introduced by surface movement or deformation will be seen as three-dimensional (3-D) surface deformation in the temporally mixed stereogram of Google Maps and Microsoft Bing Maps image data. Occasionally, screen shots have to be rotated in such a way that the flow direction is approximately parallel to the eye base of the observer. A first guess of the flow direction can be easily obtained by topographic glues and by shape and structure of the rock glacier, respectively. Finally, three highly active rock glaciers, i.e., Leibnitzkopf, Tschadinhorn, and Ganot, were selected for detailed analysis (see **Fig. 1**). These rock glaciers are listed as 'is 210b', 'is 185', and 'is 192' in the rock glacier inventory of central and eastern Austria compiled by *Lieb*, *Kellerer-Pirklbauer* and *Kleinferchner (2010)*. According to this inventory, all three rock glaciers are classified as intact. The inventory also provides geomorphometric parameters, such as lower limit of the rock glacier, max. length, max. width, etc., of all rock glaciers. Concerning the kinematic state of the three rock glaciers, we can find some qualitative information in *Buchenauer (1990: 135, 210, 178)*. In the following subsections the three rock glaciers are described briefly.

3.2. Leibnitzkopf rock glacier

Leibnitzkopf rock glacier (46°55'51" N, 12°42'43" E, see **Fig. 1**) is located at the head of Leibnitz valley, south of Gartl lake. The rock glacier lobe has a max. length of 350 m and a max. width of 200 m. Its lower limit is at approx. 2450 m. The main flow direction is from east to west with at least two distinct debris supply channels originating from the steep slopes of Törlkopf (2755 m) and Leibnitzkopf (2863 m). The confining frontal and marginal slopes are well developed and steep. *Buchenauer (1990)* assessed Leibnitzkopf rock glacier as being most probably inactive.

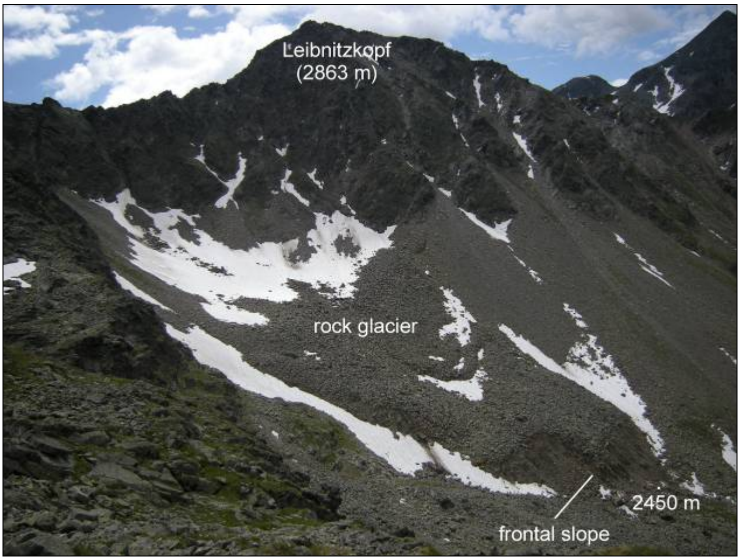

Fig. 2 Terrestrial view of Leibnitzkopf rock glacier. Viewing direction in southeasterly direction (*Photograph taken by V. Kaufmann on 21 July 2009*)

3.3. Tschadinhorn rock glacier

Tschadinhorn rock glacier (46°59'40" N, 12°42'13" E, see **Fig. 3**) is an impressive, approx. 600 m long, tongue-shaped creep phenomenon which has its root zone below the steep, northwest facing rock faces of Tschadinhorn (3017 m). Characteristically, the rock glacier tongue is moving over a prominent terrain ridge into steeper terrain of a small valley. Since the snout of the rock glacier, its lower limit extents to 2580 m, has advanced into a region of alpine meadows, the lower half of the rock glacier can be recognized very clearly in aerial photographs and also in nature. The width of the rock glacier at its lower part is approx. 100 m. Flow structures composed of furrows and ridges are well developed. *Buchenauer (1990)* measured the temperature of springs and carried out Schmidt-hammer seismic measurements. Based on the results obtained he deduced that permafrost is most probably existent at this site. He also concluded that the outer part of the orographic left side of Tschadinhorn rock glacier is inactive, and therefore not taking part in the downslope movement.

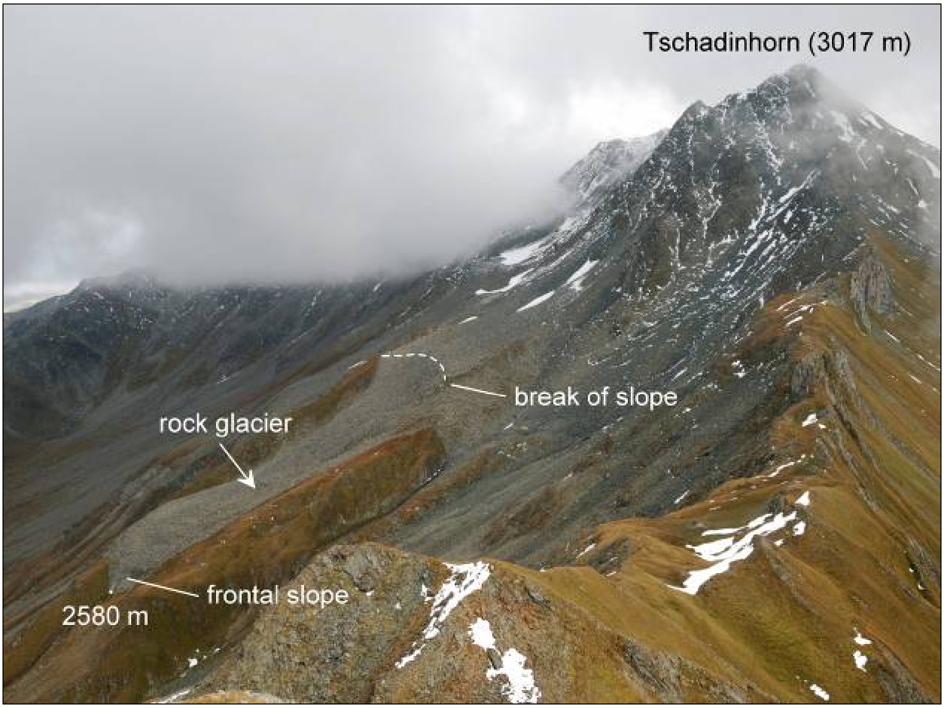

Fig. 3 Terrestrial view of Tschadinhorn rock glacier as seen from Schönleitenspitze (2809 m). Viewing direction in northeasterly direction
(*Photograph taken by V. Kaufmann on 20 September 2009*)

3.4. Ganot rock glacier

Ganot rock glacier (46°57'45" N, 12°41'54" E) is located in the Ralf valley northwest of Ganot (3102 m) and it is also a quite long (max. length of 450 m) tongue-shaped flow structure. Morphologically, this rock glacier is much more hidden compared to Tschadinhorn because it structurally follows a small elongated cirque floor. The front of the rock glacier tongue ends at a steep rock cliff or has even advanced further down in some parts causing rock fall and sliding. The width of the rock glacier is approx. 150 m in the lower part. Main flow direction is to the west. Based on geomorphological evidence, spring temperatures and Schmidt-hammer seismic measurements *Buchenauer (1991)* concluded in his doctoral thesis that permafrost is present and the rock glacier is active. Flow-like features, such as furrows and ridges, support the latter.

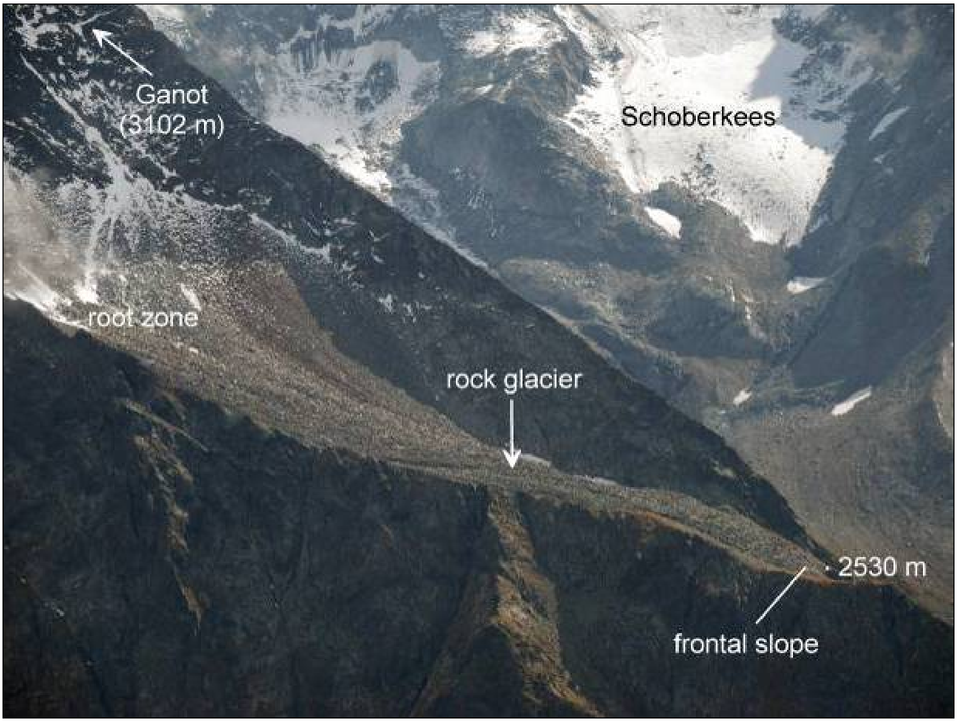

Fig. 4 Terrestrial view of Ganot rock glacier as seen from Schönleitenspitze (2809 m). Viewing direction in southsoutheasterly direction
(*Photograph taken by V. Kaufmann on 20 September 2009*)

4. GEOMETRIC CONSIDERATIONS

(1) The image geometry of screenshots (screen captures) of both virtual globes was analyzed first before working on the present test sites. At the time of investigation, it was found out that screen dumps of image data of both virtual globes had exactly the same geometry: A first detailed analysis was carried for a region where both virtual globes relayed on the some external data source. Outer Hochebenkar rock glacier (46°50'01" N, 11°00'30" E), Ötztal valley, the Tyrol, was taken as a suitable test site (cp. also *Kaufmann and Ladstädter, 2003*).

The high-resolution color orthophotos of both virtual globes originate from the Austrian Federal Office of Metrology and Surveying (BEV) in Vienna. The photographs were taken on 5 September 2003 at 1:17,000 image scale. (Remark: The author had already worked with this image source in a prior project.) Screenshots of the area of interest were made from each of the two globes at various resolutions. At the time of investigation, the zoom levels in both systems were identical and amounted to 20 cm, 40 cm, 80 cm, 160 cm, etc. ground sampling distance (GSD). GSD was derived from the scale bar shown in the respective Geobrowser window. In a later stage of the study both virtual globes switched to 17.5 cm, 35 cm, 70 cm, 140 cm, etc. GSD. All layers of the multi-resolution data set available were registered by dense matching. The screenshots of Google Maps served as a reference. The results of the image registration are presented in **Table 1**.

Table 1. ***Results of the relative image registration of screenshots of Google Maps and Microsoft Bing Maps covering Outer Hochebenkar rock glacier, the Tyrol. Images were captured at sizes of approx. 1280 pixel × 700 pixel. Grid spacing: 25×25 pixel. Template size: 51×51 pixel***

Google Maps GSD (cm)	Microsoft Bing Maps GSD (cm)	number of points	easting r.m.s.e (pixel)	northing r.m.s.e (pixel)	mean NCC coefficient	mean back matching distance (pixel)
20	20	1228	±0.44	±0.56	0.941	0.05
40	40	1213	±0.19	±0.31	0.912	0.02
80	80	1244	±0.10	±0.12	0.878	0.02
160	160	1260	±0.08	±0.08	0.859	0.03

Results obtained show that corresponding screenshots of both virtual globes can be registered perfectly well within sub-pixel accuracy which relates to a horizontal measuring accuracy of approx. ±10 cm for both easting and northing. This means that the image geometries of both virtual globes can be considered the same, at least for small areas looked at highest zoom levels using standard large monitors (desktops).

(2) Furthermore, it was confirmed by measurements that both virtual globes present their image/map data in the well-known Mercator projection at the end user's desktop. Mercator projection is a conformal cylindrical map projection. Conformality is obtained by appropriate scale change (1/cosφ) in north-south direction. **Table 2** provides an empirical proof that the map projection used in Microsoft Bing Maps is indeed a Mercator projection. Because of the finding of **(1)** this statement also holds for Google Maps.

Table 2. ***Proof that Microsoft Bing Maps uses Mercator map projection***

latitude φ(°)	image scale derived from scale bar	quotient q (scale change)	computed latitude φ(°) (φ=cos^{-1}q)
0	1 pixel = 130.8 m	1	0
47	1 pixel = 89.4 m	0.683	46.88
60	1 pixel = 65.5 m	0.500	59.95
80	1 pixel = 22.82 m	0.174	79.95

(3) The last pre-study also relates to Google/Microsoft image data covering the same area, which, however, differs in date and time. Our test site is now Hinteres Langtalkar rock glacier (46°59'11" N, 12°46'49" E) located in the western part of the Schober group. The original photographs of the data providers to the virtual globes were made available to the author in a prior study (cp. *Kaufmann and Ladstädter, 2003*). Orthophotos of two time periods associated with the two virtual globes were produced in-house using high-resolution digital terrain models (DTMs). Map projection of the in-house orthophotos is Gauss-Krüger projection (system M31). In this last geometric test screenshots of both virtual globes were registered to the in-house derived orthophotos. Automatic image registration was carried out at a nominal GSD of 80 cm in order to cover a larger area, i.e., 1200 m × 700 m. Three linear 2-D geometric transformations were applied, i.e., a 3-parameter (rigid body) transformation, a 4-parameter (similarity) transformation, and a 6-parameter (affine) transformation. The results obtained by the latter transformation are presented in **Table 3**.

Table 3. ***Comparison of map geometry (Mercator projection) of virtual globes with Gauss-Krüger projection (M31). The distance of the area of interest to the central meridian M31 is approx. 42 km. Gauss-Krüger projection is a transverse Mercator projection (scale of the central meridian is 1, Bessel ellipsoid is used)***

virtual globe	number of points	m_0 (pixel)	easting r.m.s.e (pixel)	northing r.m.s.e (pixel)	scale (easting/northing)	rotation (°) (easting/northing)
Google Maps	1121	±0.59	±0.39	±0.74	0.979/0.981	0.409/0.408
Microsoft Bing Maps	1092	±0.56	±0.37	±0.69	0.979/0.983	0.398/0.407

Following conclusions can be drawn:

(a) Screen shots of ortho-images of limited spatial extent, e.g. 1.2 km × 0.7 km at 80 cm GSD, of both virtual globes can be resampled to national map projections of universal transverse Mercator (UTM) type with sub-pixel accuracy using an affine transformation.

(b) Similar affine parameters obtained indicate that Google Maps and Microsoft Bing Maps use the same map projection. This confirms the result obtained for the test site of Outer Hochebenkar rock glacier.

(c) Image rotations calculated equal meridian convergence. The latter amounts to (minus) 0.402°.

(d) Distances measured in both virtual globes using the scale bar as a reference are approx. 2% shorter than in the respective orthophoto given in Gauss-Krüger map projection. However, at this moment this large scale difference cannot be explained. Further investigations are needed.

5. RESULTS

In this chapter results obtained for the three given test sites will be presented. Image data was accessed in March 2009. It has to be mentioned that meanwhile both providers, Google and Microsoft, have developed further their products, and therefore technical parameters may have changed. Later on during this study, for example, both providers had changed GSD from 20 cm to approx. 17.5 cm for the higher-most zoom level. For reasons of comparison some of the work was repeated, however, no significant differences in the results were found.

5.1. Leibnitzkopf rock glacier

Measurement of horizontal flow/creep vectors were carried out at two different GSD, i.e., 40 cm and 20 cm, respectively. The 40 cm screenshots cover the whole rock glacier, whereas the 20 cm zoom level provides more detailed information on a selected area.

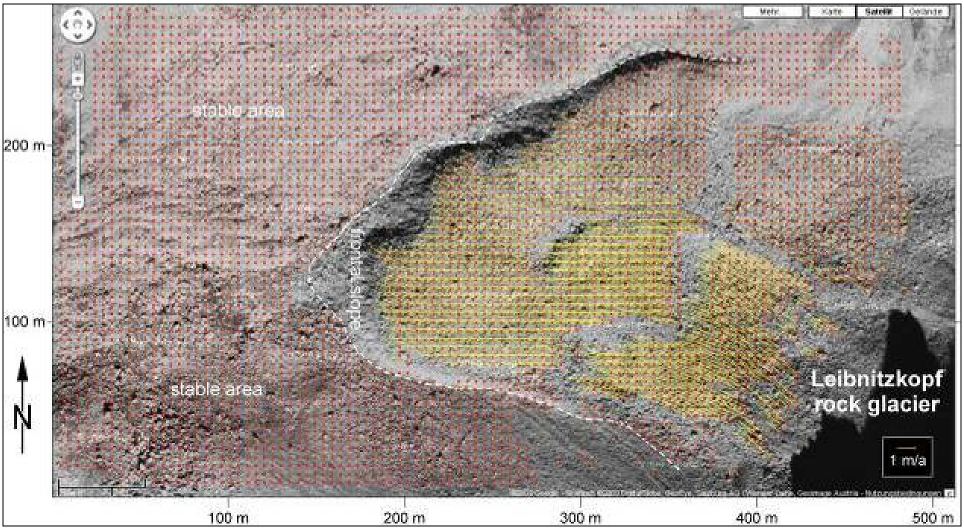

Fig. 5 Mean annual horizontal flow/creep vector field at Leibnitzkopf rock glacier. Tracking was accomplished using area-based image matching based on NCC as a similarity measure. The older orthophoto (18 September 2002) stems from Google Maps, the younger one (21 September 2006) from Microsoft Bing Maps. GSD is at 40 cm. Window size of template: 25×25 (= 10m × 10m), grid spacing: 12×12 (=4.8m × 4.8m), min. NCC coefficient: 0.4, max. back matching distance: 1 pixel

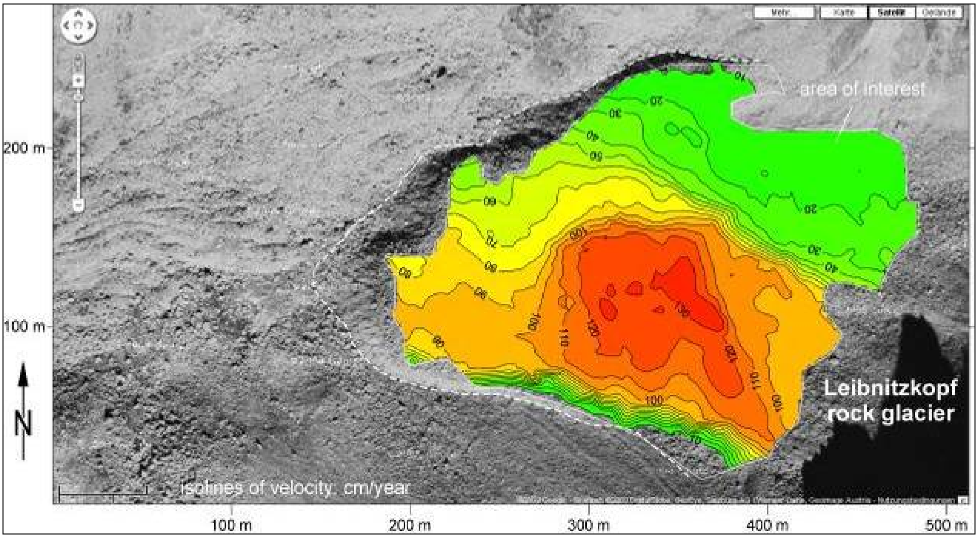

Fig. 6 Thematic map showing isolines of mean annual horizontal flow/creep velocity of Leibnitzkopf rock glacier for the time period 2002-2006. Estimated accuracy of the flow/creep velocity is ±5.1 cm/year. The maximum flow/creep velocity amounts to 137 cm/year

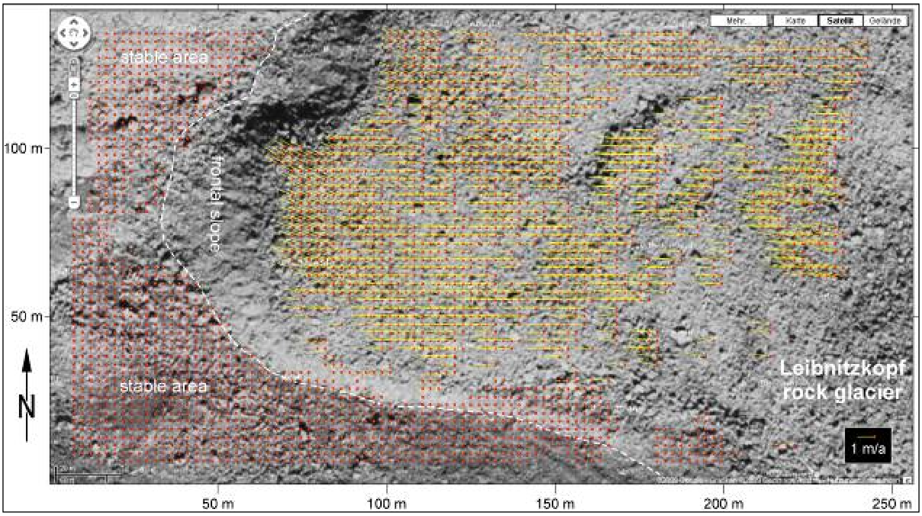

Fig. 7 etail study of Leibnitzkopf rock glacier showing mean annual horizontal flow/creep vector field for the time period 2002-2006. The older orthophoto (18 September 2002) stems from Google Maps, the younger one (21 September 2006) from Microsoft Bing Maps. GSD is at 20 cm. Window size of template: 51×51 (= 10.2m x 10.2m), grid spacing: 12×12 (=2.4m x 2.4m), min. NCC coefficient: 0.4, max. back matching distance: 1 pixel

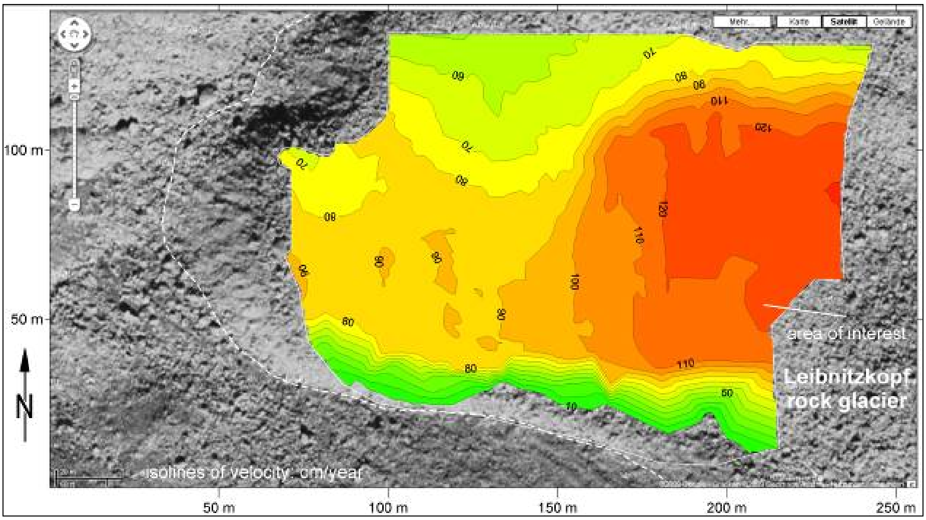

Fig. 8 Thematic map showing isolines of mean annual horizontal flow/creep velocity of Leibnitzkopf rock glacier for the time period 2002-2006. Estimated accuracy of the flow/creep velocity is ±4.2 cm/year. The maximum flow/creep velocity amounts to 133 cm/year

Discussion: The maximum mean annual flow/creep velocity at Leibnitzkopf rock glacier amounts to 137 cm/year for the time period 2002-2006. The pattern of the flow vectors suggests that the rock glaciers consists of al least two or three sub-units of different kinematic state.

5.2. Tschadinhorn rock glacier

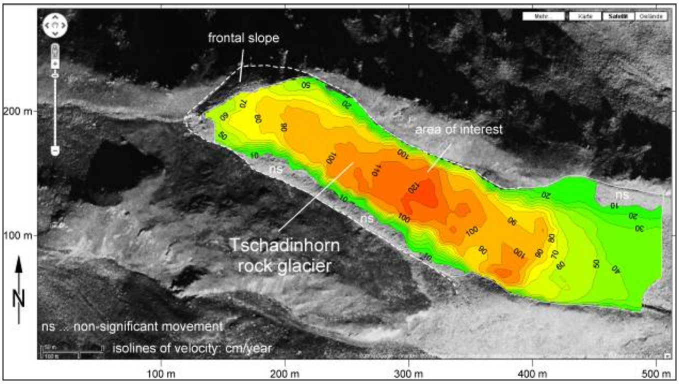

Fig. 9 Thematic map showing isolines of mean annual horizontal flow/creep velocity of Tschadinhorn rock glacier for the time period 2002-2006. Estimated accuracy of the flow/creep velocity is ±9.0 cm/year. The maximum flow/creep velocity amounts to 124 cm/year. Multi-temporal orthophotos date from 18 September 2002 (Google Maps) and 21 September 2006 (Microsoft Bing Maps). GSD is at 40 cm. Window size of template: 25×25 (= 10m × 10m), grid spacing: 12×12 (=2.4m × 2.4m), min. NCC coefficient: 0.4, max. back matching distance: 1 pixel

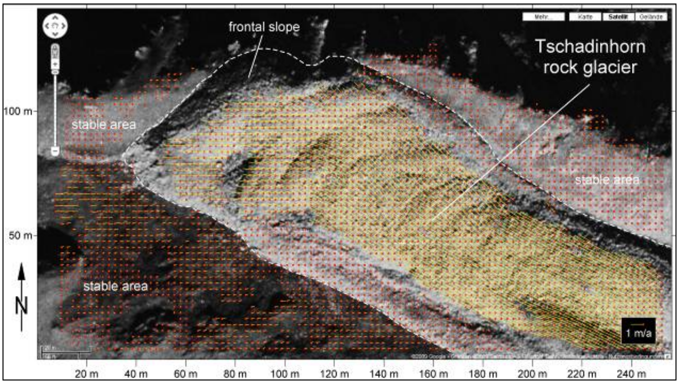

Fig. 10 Detail study of Tschadinhorn rock glacier showing mean annual horizontal flow/creep vector field for the time period 2002-2006. GSD is at 20 cm. Estimated accuracy of the flow/creep velocity is ±5.1 cm/year. The maximum flow/creep velocity amounts to 120 cm/year. Window size of template: 25×25 (= 5m × 5m), grid spacing: 12x12 (=2.4m × 2.4m), min. NCC coefficient: 0.6, max. back matching distance: 1 pixel

Discussion: The accuracy of the flow/creep velocity of the 20 cm data shown in **Fig. 10** is about 5.1 cm/year. The same value amounts to 10-15 cm/year in areas with steep terrain. The velocity vector field of **Fig. 10** also reveals that the geometric quality of the orthophotos involved is not as optimal as compared to the Leibnitzkopf example. Inaccurate DTMs cause geometrically wrong orthophotos. Errors can be detected in the process of co-registration. Displacement vectors within the limits of stable areas should have zero length by definition. Movement detected in stable areas is therefore apparent and most probably due to geometric errors of the orthophotos involved.

Fig. 9 and **10** reveal very nicely that Tschadinhorn rock glacier is flowing over a ridge into steeper terrain with significant speed-up of flow/creep velocity. The maximum velocity of 124 cm/year is reached below this ridge right in the center of the rock glacier (*Drantsch , 1997*). Flow kinematics of the active part of the rock glacier is reflected through furrows and ridges at the rock glacier surface. This very active unit is confined by an older, inactive one. The latter has a levee-type structure.

5.3. Ganot rock glacier

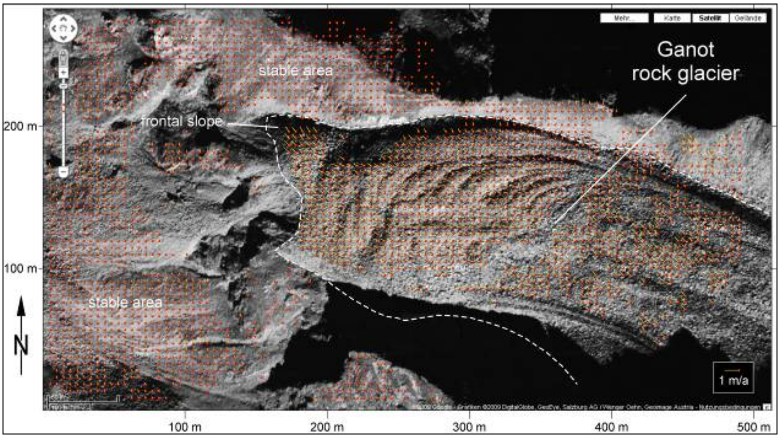

Fig. 11 Mean annual horizontal flow/creep vector field at Ganotrock glacier. Tracking was accomplished using area-based image matching based on NCC as a similarity measure. The older orthophoto (18 September 2002) stems from Google Maps, the younger one (21 September 2006) from Microsoft Bing Maps. GSD is at 20 cm. Window size of template: 25×25 (= 5m x 5m), grid spacing: 12×12 (=2.4m × 2.4m), min. NCC coefficient: 0.6, max. back matching distance: 1 pixel

The third rock glacier is of much lower activity because velocities measured in the lower third of the rock glacier do not exceed 46 cm/year. Due to the general steep terrain the overall geometric quality of the orthophotos involved is significantly lower compared to the two previous examples which resulted in flow/creep accuracies in the range of 6-10 cm/year. Highest velocities are measured close to the centerline.

6. COMPUTER ANIMATIONS

The spatio-temporal change of the surface topography of all three rock glaciers can be effectively visualized by means of computer animation. Various methods of computer animation are highlighted, for example, in Drantsch (1997). The screenshots of Microsoft Bing Maps were resampled to match exactly the reference geometry of the screenshots of Google Maps. These co-registered data sets (2 epochs each) were taken as key frames forming animated GIFs. Please see:

http://www.geoimaging.tugraz.at/viktor.kaufmann/animations.html,

for online demonstrations.

Motion parallaxes can also be recognized stereoscopically as shown in **Fig. 12**.

Fig. 12 Multi-temporal (pseudo) stereogram of Leibnitzkopf rock glacier. Left stereopartner (orthophoto, 18 September 2002) taken from Google Maps. Right stereopartner (orthophoto, 21 September 2006) taken from Microsoft Bing Maps. Parallaxes introduced by motion can be perceived stereoscopically as “hills” and “valleys” depending on the direction of motion. The main flow/creep direction has to be parallel to the eye base of the observer

7. CONCLUSIONS AND OUTLOOK

Admittedly, both virtual globes, i.e., Google Maps and Microsoft Bing Maps, still lack of high-resolution image data for many parts of the Earth. This is especially true for high mountain areas. Even if high-resolution image data is available, image acquisition dates are not appropriately enough communicated. However, this may change in the near future as soon as new image data will come up and supersede the old one. The old image data will become “historical” data, and most likely will be made available to the user. Time (as the 4th dimension) will become an issue in information retrieval.

In general, “virtual globe” stands for any kind of web-enabled GIS or Geobrowser which provides orthophotos either free of charge or at low costs or on a commercial basis. Change detection is an important task in environmental monitoring. This task can strongly benefit from image-based methods such as that one presented in this paper. The proposed method can be easily implemented, is cheap and also reliable, provided that multi-temporal orthophotos, either of airborne or space-borne type, are available at high resolution and proper metadata (acquisition date) is provided.

Quality control using sufficiently large stable areas is of great importance. This means that the geometric quality of the multi-temporal orthophotos can be checked within the proposed procedure of change detection. The procedure outlined in this paper also applies to other mass movements, such as landslides or debris-covered glaciers.

This paper has clearly shown that rock glaciers with a mean annual flow/creep velocity greater than 10-15 cm/year can be detected successfully using multi-year high-resolution orthophotos of virtual globes (Geobrowsers), such as Google Maps and Microsoft Bing Maps. Based on the results obtained Leibnitzkopf rock glacier was selected for further analysis of its kinematics using GPS measurements.

Acknowledgments
The author is grateful to his colleague A. Kellerer-Pirklbauer-Eulenstein, who helped to access the digital database of the rock glacier inventory provided by the Institute of Geography and Regional Science, University of Graz.

REFERENCES

Baltsavias E.P., (1996), *Digital ortho-images – a powerful tool for the extraction of spatial- and geo-information,* ISPRS Journal of Photogrammetry & Remote Sensing, 51(2), pp. 63-77.

Barsch D., (1996), *Rockglaciers. Indicators for the Present and Former Geoecology in High Mountain Environments*, Springer Series in Physical Environment, 16, Springer, 331 pages.

Bischof H., Leberl F., (2004). *In: McGlone, J.Ch., Mikhail, E.M., Bethel, J. and Mullen, R. (Eds.), Manual of Photogrammetry*. Chapter 5 ***Digital Image Processing***. American Society for Photogrammetry and Remote Sensing, Bethesda, Maryland, pp. 399-454.

Buchenauer H.W., (1990), *Gletscher- und Blockgletschergeschichte der westlichen Schobergruppe (Osttirol)*, Marburger Geographische Schriften, 117, Philipps-Universität Marburg, in German, 276 pages.

Dransch D., (1997), *Computer-Animation in der Kartographie – Theorie und Praxis,* Springer-Verlag, Berlin, in German, 145 pages.

Kääb A., Isakowski Y., Paul F., Neumann A., Winter R., (2003*), Glaziale und periglaziale Prozesse: Von der statischen zur dynamischen Visualisierung*, Kartographische Nachrichten, 53(5), in German, pp. 206-212.

Kääb A., (2005), *Remote Sensing of Mountain Glaciers and Permafrost Creep,* Schriftenreihe Physische Geographie – Glaziologie und Geomorphodynamik, 48, Geographisches Institut, Universität Zürich, 264 pages.

Kaufmann V., Ladstädter R., (2003), *Quantitative analysis of rock glacier creep by means of digital photogrammetry using multi-temporal aerial photographs: two case studies in the Austrian Alps,* In: Phillips, M., Springman, S.M. and Arenson, L.U. (Eds.), Permafrost, Proceedings, 8th International Conference on Permafrost, Vol. 1, Zurich, Switzerland, Swets & Zeitlinger Publishers, pp. 525-530.

Kaufmann V., (2009), *Detection and measurement of highly active rock glaciers using multi-temporal high-resolution orthophotos of virtual globes, such as Google Maps and Microsoft Virtual Earth/ Bing Maps,* International Workshop "Glacier Hazards, Permafrost Hazards and GLOFs in Mountain Areas: Processes, Assesment, Prevention, Mitigation", University of Natural Resources and Applied Life Sciences, Vienna, 10-13 November 2009, poster, http://www.geoimaging.tugraz.at/viktor.kaufmann/GAPHAZ2009_Kaufmann_Poster.pdf (accessed 9 June 2010).

Lieb G.K., (1986), *Die Blockgletscher der östlichen Schobergruppe (Hohe Tauern, Kärnten)*, Arbeiten aus dem Institut für Geographie der Karl-Franzens-Universität Graz, 27, Festschrift für Wilhelm Leitner, in German, pp. 123-132.

Lieb G.K., Kellerer-Pirklbauer A., Kleinferchner H., (2010), *Polygon basiertes Blockgletscherinventar von Zentral- und Ostösterreich erstellt im Rahmen des EU-Projektes PermaNET – Permafrost long-term monitoring network*, Graz, 2010 (accessed 8 June 2010).